Modelling and simulation of VMD desalination process by ANN

Wensheng Cao [a,d,e], Qiang Liu [c], Yongqing Wang [a,d,e], Iqbal M. Mujtaba [b,*]

[a] College of Mechanical and Energy Engineering, Jimei University, Xiamen 361021, China

[b] School of Engineering and Informatics, University of Bradford, West Yorkshire, Bradford BD7 1DP, UK

[c] School of Statistics, Capital University of Economics and Business, Beijing 100070, China

[d] Fujian Province Key Lab of Energy Cleaning Utilization and Development, Jimei University, China

[e] Cleaning Combustion and Energy Utilization Research Center of Fujian Province, Jimei University, China

* Corresponding author. E-mail address: I.M.Mujtaba@bradford.ac.uk (Prof. I.M. Mujtaba).

Abstract

In this work, an artificial neural network (ANN) model based on the experimental data was developed to study the performance of vacuum membrane distillation (VMD) desalination process under different operating parameters such as the feed inlet temperature, the vacuum pressure, the feed flow rate and the feed salt concentration. The proposed model was found to be capable of predicting accurately the unseen data of the VMD desalination process. The correlation coefficient of the overall agreement between the ANN predictions and experimental data was found to be more than 0.994. The calculation value of the coefficient of variation (*CV*) was 0.02622, and there was coincident overlap between the target and the output data from the 3D generalization diagrams. The optimal operating conditions of the VMD process can be obtained from the performance analysis of the ANN model with a maximum permeate flux and an acceptable *CV* value based on the experiment.

Keywords:

Vacuum membrane distillation; Desalination; Artificial neural network; Simulation; Modelling

1. Introduction

Membrane distillation (MD) has been the focus of worldwide academic studies as an attractive separation process by many theoreticians and experimentalists. Four

different systems of MD have been categorized depending on the process configurations as direct contact membrane distillation (DCMD), air gap membrane distillation (AGMD), sweep gas membrane distillation (SGMD) and vacuum membrane distillation (VMD). Among above systems, VMD proves to be very promising and adopts an effective way to increase membrane permeability. Applying a continuous vacuum [1] below the equilibrium vapor pressure, the air is removed from its pores in the permeate side. VMD can be applied not only for seawater desalination, but also for other areas such as ethanol recovery, removal of trace amount of contaminants and volatile organic compounds (VOCs) from water [1, 2].

In VMD configuration, transport mechanisms of vapor molecules across the membrane are described by some models such as dusty-gas model [2-4] and Schofield's model [2], Ballistic model [5], Monte Carlo model [6], velocity slip model [7], including one-dimensional [8,9] and two-dimensional models [10]. Chiam [11] offered a comprehensive review of VMD. In fact, the molecular diffusion models (analytical) have the advantage of giving some deterministic insights on the process. However, the analytical models are often complex and sue of such models to find out the optimum operating conditions of the studied process proves difficult. To overcome this drawback, a different type of model based on artificial neural networks (ANN) can be considered for the optimization of the process under study [12].

ANN based models can deal with non-linear multivariate regression problems. This type of model is not dependent on explicit expressions of the physical meaning of the process or system under investigation but is dependent on input-output relationship of the process and is often referred to as ‘‘black-box’’ models [13, 14]. The ANN models can be easily developed using experimental data from a process by applying Design of Experiments techniques [12]. ANN modeling has been extensively applied in different fields of science, medicine and technology [12-15].

In this study, we develop an ANN based model for VMD process, and use the model for the optimization of the operating conditions of the process via simulation.

2. Theory

ANN consists of neurons being connected in a systematic way which can map input and output data [13-16]. The connections include strengths (or weights) and threshold values (or biases). With regard to the model of a single neuron, any scalar input x_i (either from original data, or from the output of other neurons in the neural network) is conveyed via a connection by multiplying its strength of the scalar weight

w_i to produce the product ($x_i \times w_i$). The bias b is a threshold value, besides being a constant input of unity and is simply added to the product ($x_i \times w_i$) by summing junction. The summing junction of a particular neuron aggregates ($x_i \times w_i$) and b into a net input λ that may be expressed as [15, 17]:

$$\lambda = \sum_{i=1}^{n} x_i \times w_i + b \qquad (1)$$

where $x_i (i = 1, 2, \cdots, n)$ denotes the input variable, i is the integer index, n is the number of input variables, w_i is the connection weight and b is the bias.

The activation signal goes through a function known as a transfer function which takes the net input to produce the output of the neuron. The frequently used transfer functions are the logistic function (an S-shaped sigmoid), hyperbolic tangent function, negative exponential function, and sine function [18].

Generally, the neurons are grouped into several layers consisting of hidden layers and an output layer. The most frequently used network topology is the multi-layer feed-forward topology, also referred to as multilayer perceptrons (MLP) [13, 17, 18]. During the network training process, the weights and biases of the network are updated systematically so that it can forecast the output for a given set of inputs [12]. Amongst many training algorithms, the frequently used training algorithm is the back propagation (BP) which is based on gradient descent method. The network training by BP algorithm includes an iterative optimization process where the weights and biases are adjusted while minimizing a performance function such as mean squares error MSE [12]. The MSE may be defined as:

$$\mathrm{MSE} = \frac{1}{N} \sum_{j=1}^{N} \left(Y_{j,\mathrm{target}} - \hat{Y}_{j,output} \right)^2 \qquad (2)$$

where $Y_{j,\mathrm{target}}$ is the experimental target response, $\hat{Y}_{j,output}$ is the predicted output, N is the number of data points. A single iteration of BP algorithm may be written as [17]:

$$\mathbf{W}^{(new)} = \mathbf{W}^{(old)} - \eta \cdot \mathbf{grad}(\mathrm{MSE}) \qquad (3)$$

where **W** denotes the vector of weights and biases, **grad**(MSE) denotes the gradient of performance function and η is the learning rate.

3. Experimental

A VMD experiment was carried out in Jimei University and the data are presented in Appendix. The experimental set-up adopted a cross flow VMD module made from the Tianjin Hydroking Science and Technology Ltd (China) in this experiment. It is rectangular, with internal dimensions of 75mm long, 75mm wide and 50mm high. The membrane is hollow fiber polypropylene with nominal pore size of 0.2μm, porosity of 50-60 % and thickness of 220μm. The effective membrane area for vapor transport is 0.25m^2 [19].

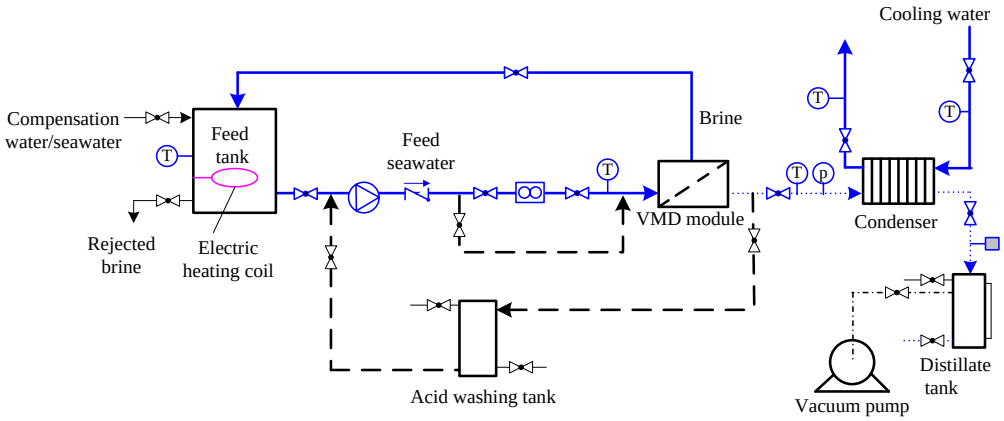

Fig. 1 VMD experimental set-up [19]

The experimental set-up is shown schematically in Figure 1. The dotted line showing the acid washing loop for membrane cleaning was included in the VMD system. Normal seawater temperature is below 40 ^{o}C. The feed was heated by an electric heating coil for evaluation of the implications of rising temperatures. The effects of the fundamental operation parameters, including the feed inlet temperature, vacuum pressure, feed flow rate and feed salt concentration, on permeate flux which is the main performance index of VMD process [20], were studied experimentally. The results are presented in the Appendix. In this study, the ANN architecture consists of four inputs (Feed inlet temperature, Vacuum pressure, Feed flow rate and Feed salt concentration) and one output (Permeate flux).

4. Discussions and results by STATISTICA

In this study 38 sets of experiments were carried out applying different VMD operating conditions in order to develop the ANN model by STATISTICA software [21]. 70% of the total experimental data set was assigned for the training and 15% for the testing and 15% for the validation of the proposed ANN model. The training data is mainly used for modeling, and the parameters in the model, which are mainly the

weight values. The testing data is used in network structure determination in that a number of networks with different number of hidden neurons are developed and the one giving the best performance on the testing data is considered to have the appropriate number of hidden neurons. The performance of this neural network is then further evaluated on the validation data. The statistical data of the input and output variables used for training ANN model are presented in Table 1. These variables are generally needed for preprocessing before use. The data scaling method is to convert the data of each variable to a certain range of [a, b], usually within [0, 1].

The scaling way is usually used by $x_{scale} = \frac{x - x_{\min}}{x_{\max} - x_{\min}}$.

Tab. 1 Statistical data of the input and output variables

Variables	Range	Mean±S.D.
Input variables		
Feed inlet temperature (^{o}C)	60~70.44	65.22±7.38
Vacuum pressure (MPa)	0.037~0.089	0.063±0.037
Feed flow rate (L/h)	69.89~111	90.45±29.07
Feed salt concentration (g/kg)	30~45	37.5±10.6
Output variable		
Permeate flux (kg/m^{2}h)	0.2~14.6	7.4±10.2

In this study, the number of hidden layers and neurons was decided based on training different feed-forward networks of various architectures and selecting the optimal architecture which gives minimum value of MSE. The optimal architecture in this study was found to be a feed forward neural network with 4 inputs, one hidden layer with 3 neurons and one output layer with a single neuron (Fig. 2).

The hidden layer neurons have hyperbolic tangent transfer function (Tanh) and the output layer neuron has sigmoid transfer function (logistic). Fig. 2 shows that the connections consist of weights (biases not shown) between inputs and neurons of different layers. In this work, the network ANN (4:3:1) has been trained using BP method based on BFGS algorithm. BFGS performs significantly better than the more traditional algorithms such as Gradient Descent method [18]. Table 2 shows the optimised values of weights and biases.

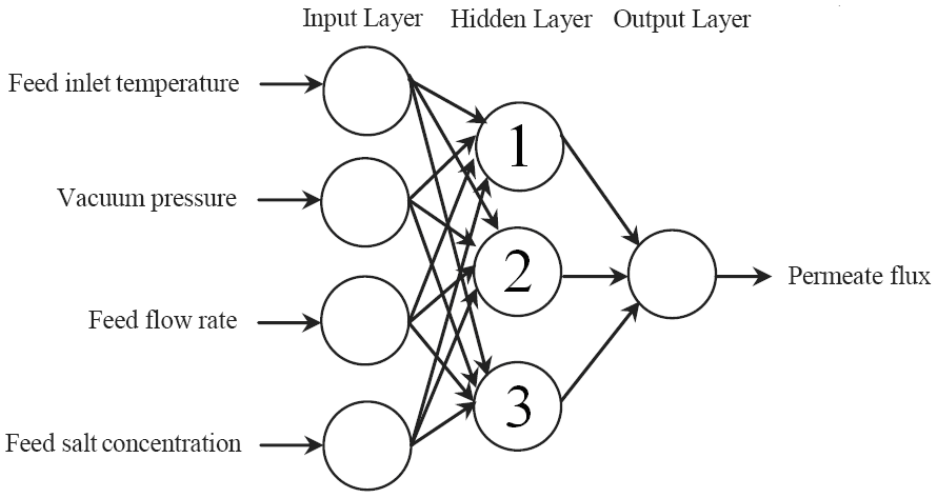

Fig. 2 Optimal architecture of ANN used for prediction of the VMD performance index

Tab. 2 Optimal values of weights and biases for the ANN model

Weight ID	Connections MLP 4-3-1	Weight Values
1	Feed inlet temperature --> hidden neuron 1	2.01514
2	Vacuum pressure --> hidden neuron 1	2.13883
3	Feed flow rate --> hidden neuron 1	0.22878
4	Feed salt concentration --> hidden neuron 1	0.17985
5	Feed inlet temperature --> hidden neuron 2	0.37488
6	Vacuum pressure --> hidden neuron 2	-1.71149
7	Feed flow rate --> hidden neuron 2	-0.52978
8	Feed salt concentration --> hidden neuron 2	0.14996
9	Feed inlet temperature --> hidden neuron 3	-1.51574
10	Vacuum pressure --> hidden neuron 3	-2.04351
11	Feed flow rate --> hidden neuron 3	0.16470
12	Feed salt concentration --> hidden neuron 3	0.11017
13	input bias --> hidden neuron 1	-0.86055
14	input bias --> hidden neuron 2	1.13319
15	input bias --> hidden neuron 3	3.09966
16	hidden neuron 1 --> Permeate flux	1.60590
17	hidden neuron 2 --> Permeate flux	-2.41470
18	hidden neuron 3 --> Permeate flux	-3.26424
19	hidden bias --> Permeate flux	-1.37503

Following the training, the optimal values of weights and biases generates the ANN model for the VMD process, but additional steps of testing and validation are still required. Figs. 3~6 show the agreement between the ANN predicted results and the experimental data for training, testing and validation data subsets as well as for all data set (i.e. Train + Test + Validation). A linear correlation coefficient of 0.994874

was obtained for training data subset (Fig. 3). For the test subset the linear correlation coefficient was 0.998656 (Fig. 4) while for validation subset the correlation coefficient was 0.999555 (Fig. 5). These values display the goodness of fit between the predicted results given by the ANN model and all experimental data employed [12]. Therefore it is obvious that ANN model has the power of interpolating well the experimental data for VMD process.

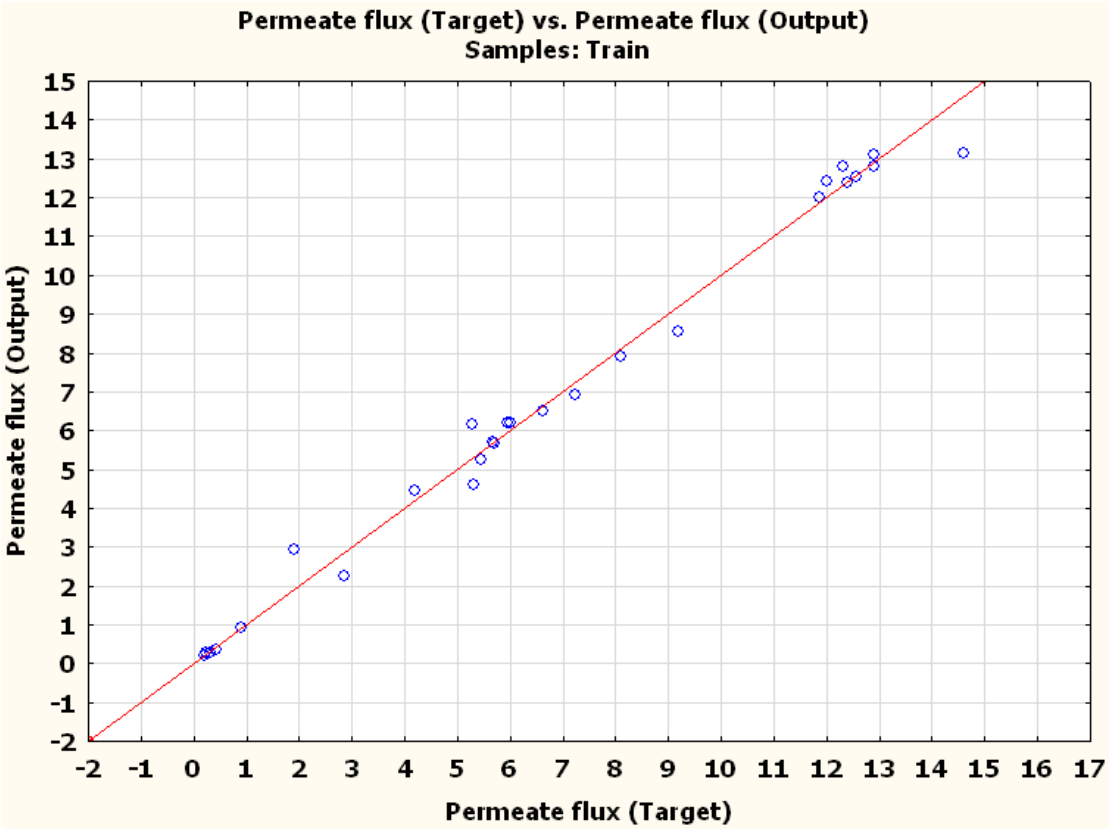

Fig. 3 Experimental VMD performance index versus predicted one for training subset

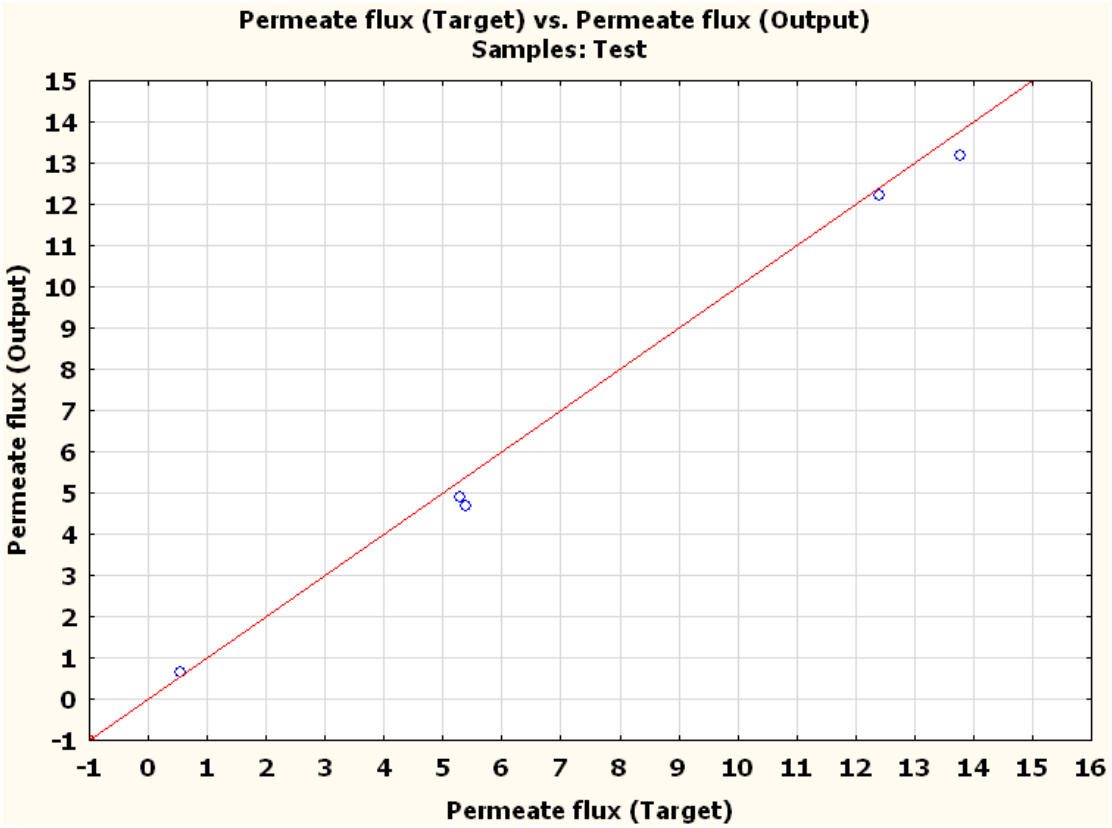

Fig. 4 Experimental VMD performance index versus predicted one for testing subset

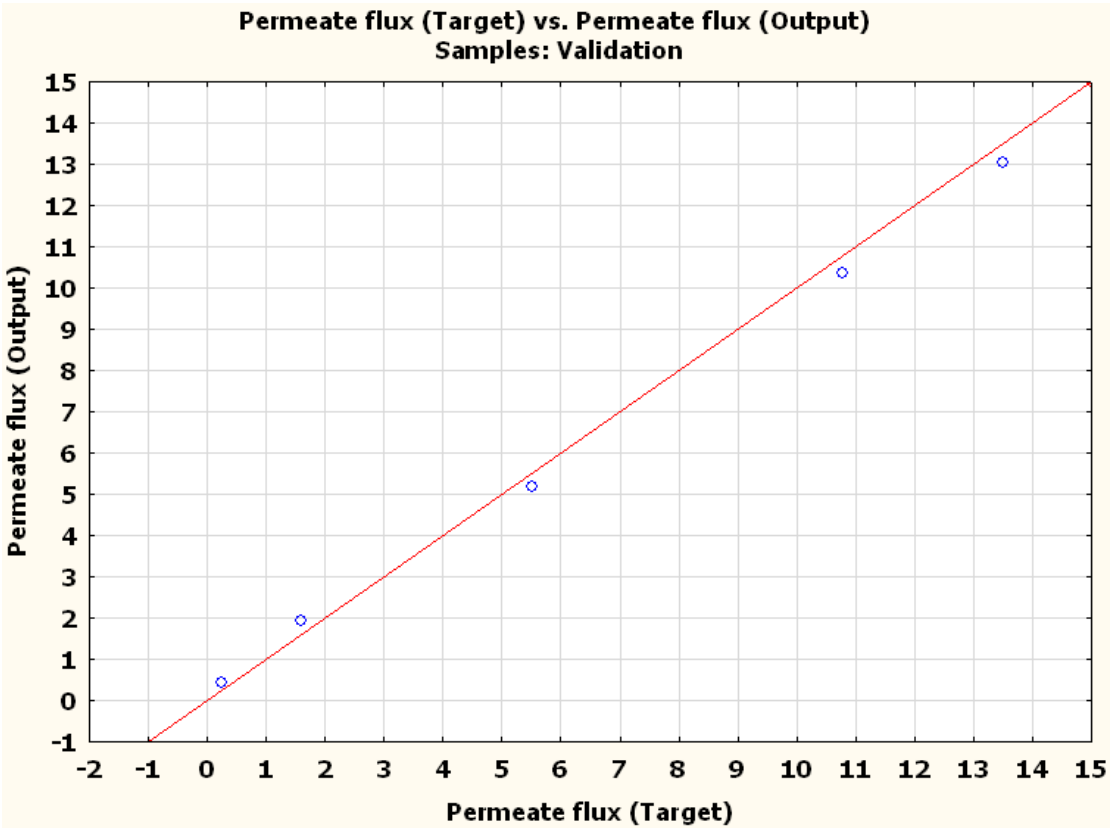

Fig. 5 Experimental VMD performance index versus predicted one for validation subset

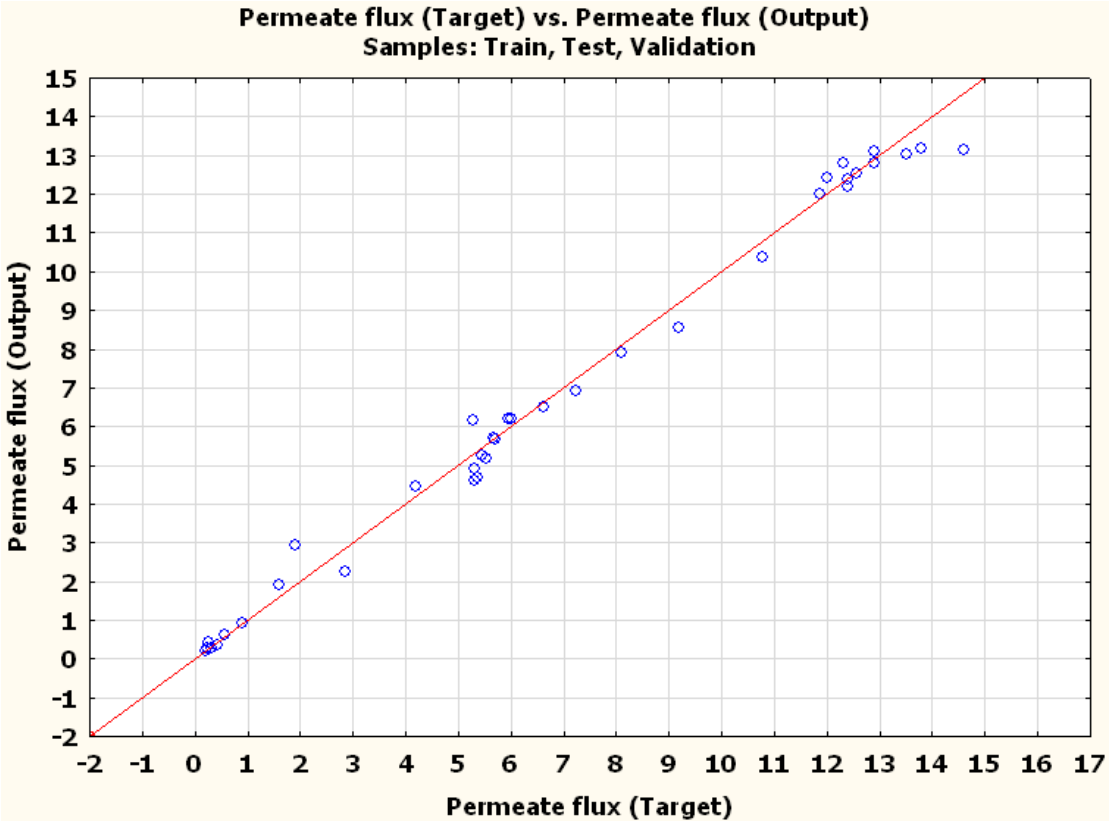

Fig. 6 Experimental VMD performance index versus predicted one for all subsets

Also, the analysis of variance was carried out to validate the ANN model statistically. The result of permeate flux residuals statistical test was shown in Fig. 7. According to this statistical test, almost all of the residual errors data were located in the yellow areas of [-1, 1.2] interval. In order to investigate whether the residual errors are reasonable or not, the coefficient of variation (*CV*) is to be introduced because it is a measure of relative variability, which equals standard deviation divided by mean. The formula is

$$CV = \frac{\sqrt{\frac{1}{n-1}\sum_{i=1}^{n}(x_i - \hat{x}_i)^2}}{\frac{1}{n}\sum_{i=1}^{n}\hat{x}_i} \qquad (4)$$

where $\hat{x}_i$ is the fitting data, x_i is the data of true values, n is the number of validation data, and $(x_i - \hat{x}_i)$ is the residual value, which means the observed value minus the predicted value. The calculation value of *CV* is 0.02622 seems to be acceptable.

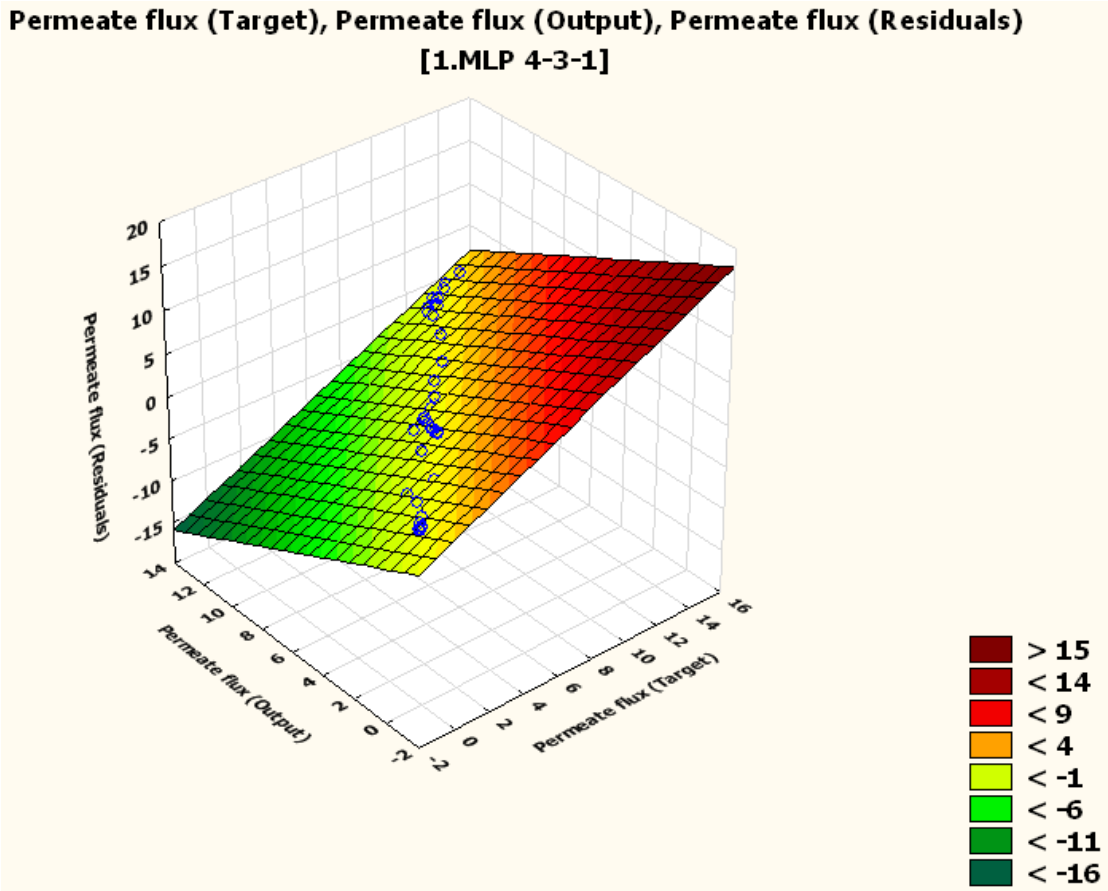

Fig. 7 3D plot of Target-Output-Residuals

Figs. 8 and 9 show the experimental and predicted VMD performance index in 3-D plots. These plots show that there was coincident overlap between the target and the output data and the proposed model is statistically valid within the experimental region.

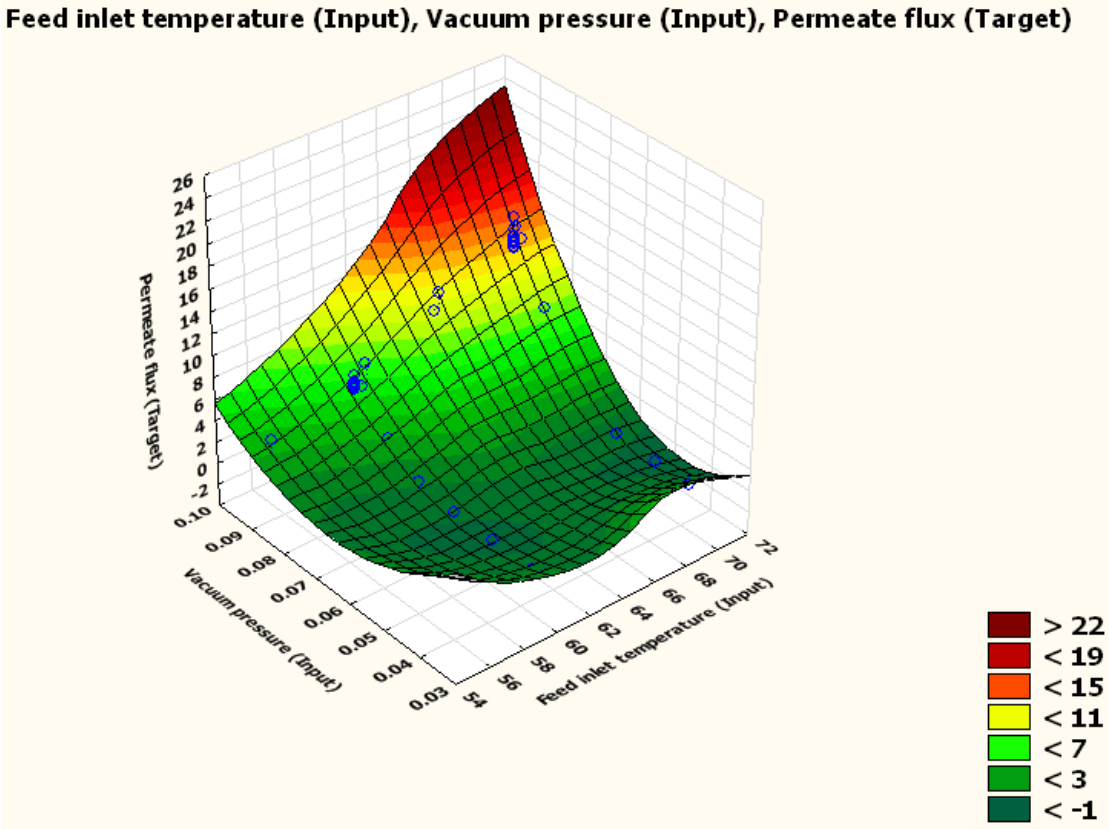

Fig. 8 3D plot of Feed inlet temperature-Vacuum pressure-Permeate flux Target

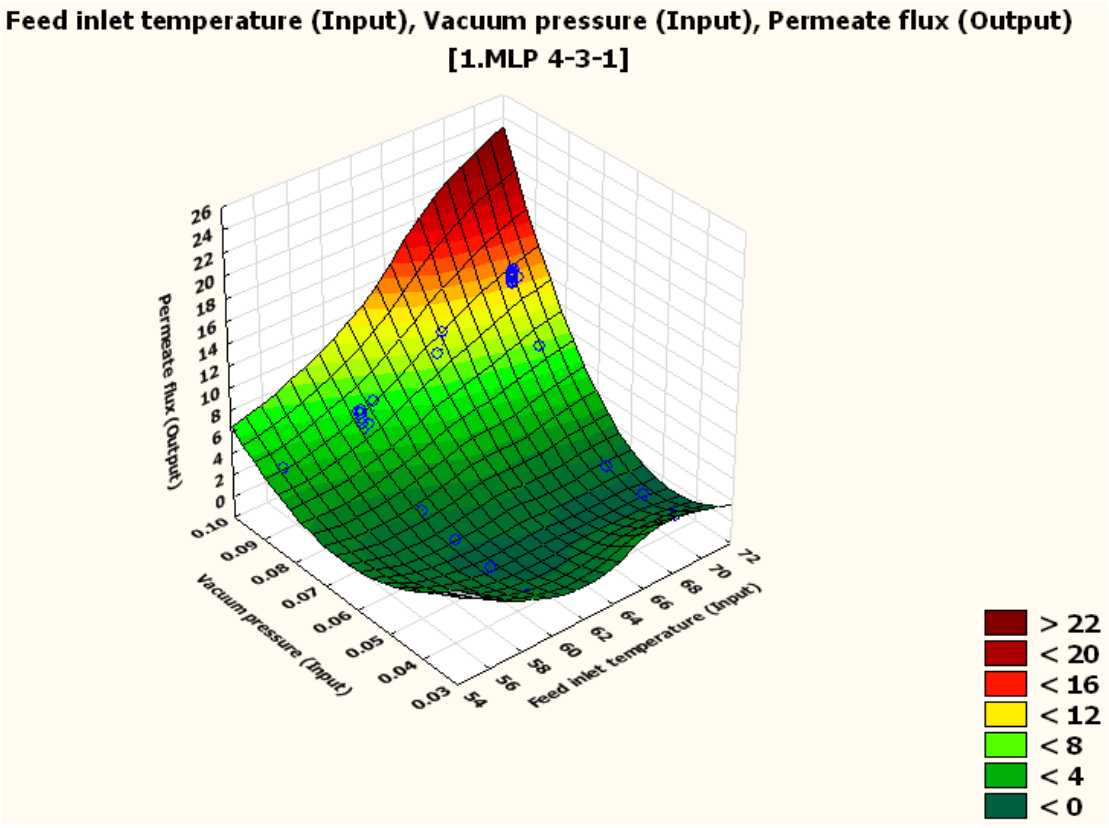

Fig. 9 3D plot of Feed inlet temperature-Vacuum pressure-Permeate flux Output

When the ANN model was constructed and passed through the processes of training, testing and validation, it has the "magic power" to predict that of unseen data for determining the optimum operating conditions. Figs. 10-13 show the generalization of the ANN model for the predicted VMD performance index for different input variables.

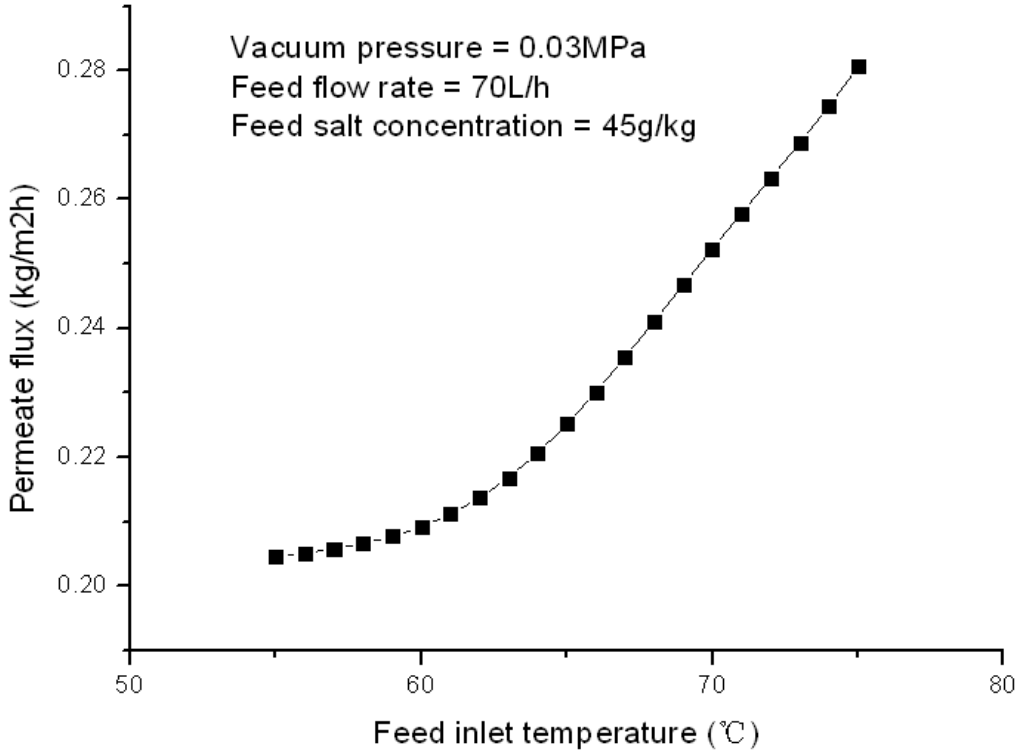

Fig. 10 Neural network generalization of the VMD performance index as a function of feed inlet temperature (55-75^{o}C)

Fig. 10 shows the effect of the feed inlet temperature on the permeate flux maintaining the other variables fixed (0.03MPa vacuum pressure, 70L/h feed flow rate and 45g/kg feed salt concentration). The increase of the feed inlet temperature yields to an increase of the performance index and this effect is more pronounced for high temperature values. The influence of feed inlet temperature is significant with increase rate of 37% from 0.20471 to 0.2806 kg/m^{2}h, although the performance index is low as the other three input variables were set to the most unfavorable conditions. Note, higher feed inlet temperature results in exponentially higher water vapor pressure at the hot side of the membrane, causing higher mass transfer driving force for vapor penetration which is in line with earlier observations [19].

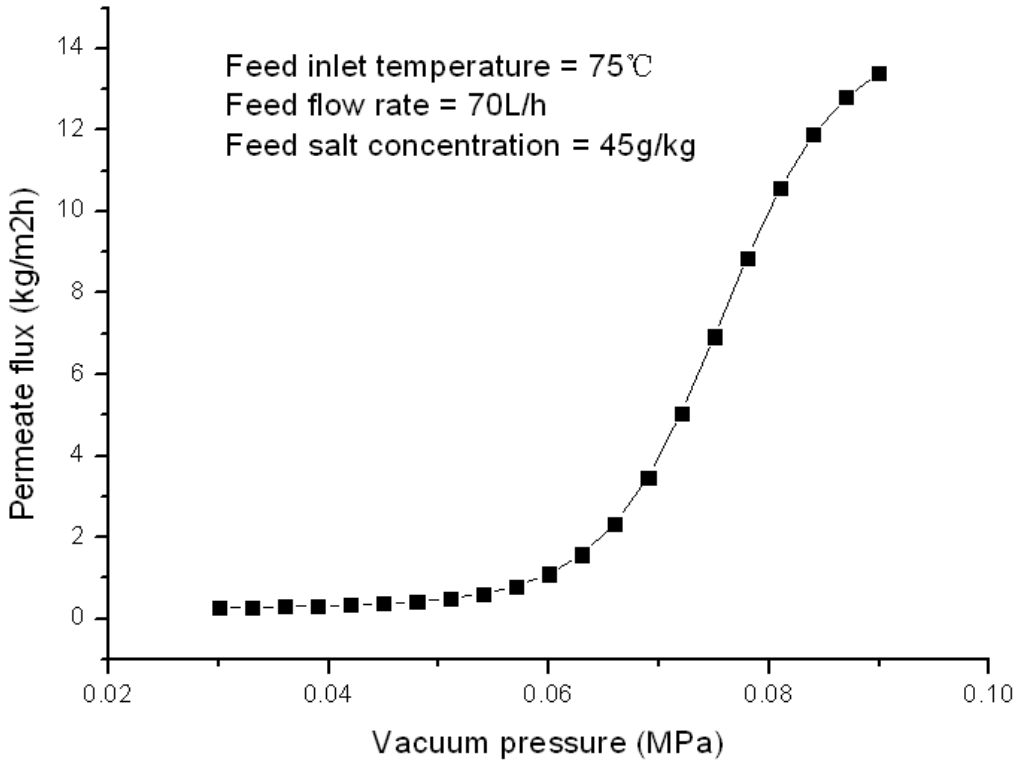

Fig. 11 Neural network generalization of the VMD performance index as a function of vacuum pressure (0.03-0.09MPa)

Fig. 11 presents the influence of the vacuum pressure on the performance index when the other variables remained fixed (75^{o}C feed inlet temperature, 70L/h feed flow rate and 45g/kg feed salt concentration). As can be seen, the increase in Vacuum pressure leads to an increase in the performance index, especially for the start of about 0.063MPa there was a sharp rise with increase rate of 748% from 1.58188 to 13.40919 kg/m^{2}h, while at the lower vacuum pressure ($<$0.063MPa) the increase rate was only 464% from 0.2806 to 1.58188 kg/m^{2}h. Kuang et al [22] attributed the phenomena to the change in vaporization behavior of the hot-side solution from surface evaporation to intense boiling, but Wang et al [19] rejected this explanation. We think the reason for this phenomena is due to the pressure difference between the hot side and the permeate side of the membrane. When the pressure difference is positive, the permeate flux rises drastically. It is clear that higher vacuum pressure (i.e. lower absolute pressure at the permeate side) should be taken to pursuit higher water production driven by the large vapor pressure difference between the two sides of the membrane.

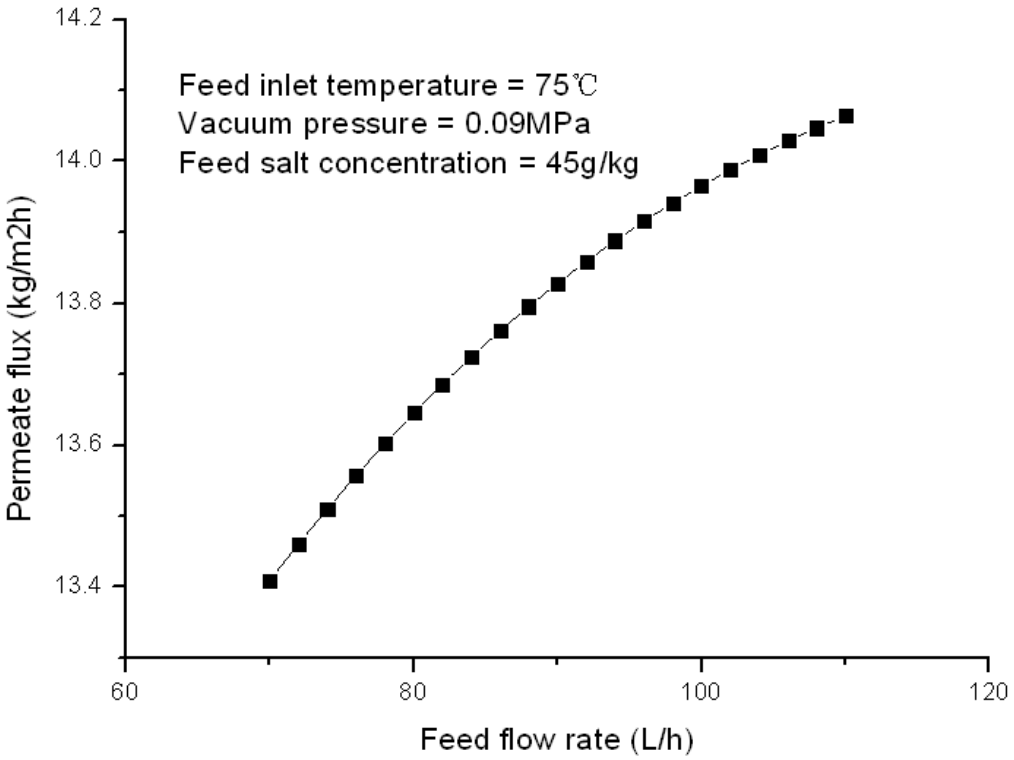

Fig. 12 Neural network generalization of the VMD performance index as a function of feed flow rate (70-110L/h)

Fig. 12 shows the dependence of the performance index on feed flow rate keeping the other conditions constant (75^{o}C feed inlet temperature, 0.09MPa vacuum pressure and 45g/kg feed salt concentration). The increasing in feed flow rate results in an increase in the performance index but this effect is weak with increase rate of 5% from 13.40919 to 14.0644 kg/m^{2}h. The increase of feed flow rate implies a higher velocity of the feed solution. This enhances the heat and mass transfer in the boundary layer on the membrane surface and reduces the effect of the temperature and concentration polarization [19].

Also, keeping the other conditions constant (75^{o}C feed inlet temperature, 0.09MPa vacuum pressure and 110L/h feed flow rate), Fig. 13 presents the effect of the feed salt concentration on the performance index. An inverse effect of feed salt concentration is observed with decrease rate of 1.4% from 14.26581 to 14.0644 kg/m^{2}h, showing weaker influence compared to that by feed flow rate. The is due to the fact that higher feed salt concentration gives lower water activity and higher concentration polarization, which result in lower water vapor pressure at the hot side of the membrane. This consequently leads to lower vapor pressure difference between the two sides of the membrane [19]. The trend is in line to that observed recently in

[23].

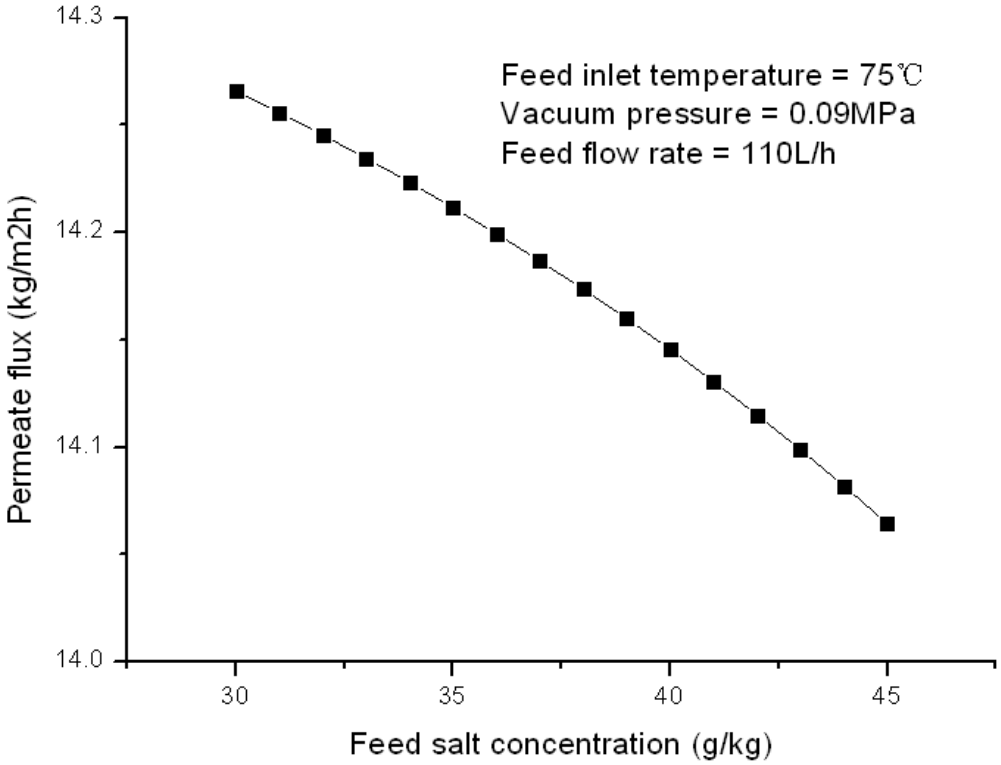

Fig. 13 Neural network generalization of the VMD performance index as a function of feed salt concentration (30-45g/kg)

According to Figures 10~13 there are interaction effects among the four input variables. Among them Vacuum pressure and Feed inlet temperature are the main factors influencing Permeate flux, which is consistent with the sensitivity analysis of the ANN model, that is 85.90244 of Vacuum pressure, 52.64689 of Feed inlet temperature, 2.017364 of Feed flow rate and 1.115243 of Feed salt concentration. So the optimum operating condition was determined by the performance analysis of the ANN model and the obtained optimal conditions were 75^{o}C feed inlet temperature, 0.09MPa vacuum pressure, 110L/h feed flow rate and 30g/kg feed salt concentration with a maximum experimental performance index of 14.266 kg/m^{2}h within the parameter range and the coefficient of variation of 0.02622.

5. Conclusions

This work was to find a way to predict accurately the unseen data for VMD process based on the experiment. A feed forward ANN model is developed for this purpose. MLP back propagation algorithm was adopted to train and determine the

optimal architecture (4:3:1) of ANN. The proposed ANN model proved to be an effective and precise tool for the prediction of the experimental data with good correlation coefficients for the permeate flux of training, testing and validation subsets. In addition, using the residual test and variance analysis, the ANN model was validated statistically. High reliability for the response prediction was found, although the amount of available experimental data used for ANN modeling was very limited (38 samples in this case).

The ANN model simulation shows that the effect of the vacuum pressure is the greatest followed by the feed inlet temperature. Using the ANN model, the VMD performance index was optimized. The resulting optimal solution represents the best VMD operating conditions within a reasonable parameter range and an acceptable *CV* value.

Acknowledgements

The author is extremely grateful to the University of Bradford, as well as the 2013 Visiting Scholar Program of Fujian Province in China, which supported the author (conferred the title of Honorary Visiting Academic) to research at the University of Bradford. This paper was financially supported by the Huang Huizhen Discipline Construction Foundation of Jimei University (ZC2012015) and Technology Project of Fujian Provincial Department of Education (JA12191). This work was also supported by the Technology Project of State Administration of Work Safety (201310180001) and Youth Outstanding Talents Cultivation Plan of Beijing Municipal Education Commission (CIT&TCD201404133).

Appendix

VMD experimental data used for ANN modeling

Case name	Sample	Feed inlet temperature (^oC)	Vacuum pressure (MPa)	Feed flow rate (L/h)	Feed salt concentration (g/kg)	Permeate flux (kg/m^2h) *Target*	Permeate flux (kg/m^2h) *Output*
1	Train	55.67	0.088	70	35	1.92	2.92953
2	Test	60.48	0.088	70	35	5.3	4.90045
3	Train	65	0.088	70	35	9.2	8.55972
4	Train	70.44	0.088	70	35	12.4	12.39903
5	Train	55	0.088	110	35	4.2	4.44830
6	Train	60.74	0.088	110	35	7.23	6.90233
7	Validation	65.29	0.088	110	35	10.77	10.35722
8	Test	70.12	0.088	110	35	13.78	13.18660
9	Train	60	0.037	90	35	0.2	0.22050
10	Train	60	0.048	90	35	0.22	0.26640
11	Validation	60	0.059	90	35	0.25	0.43242
12	Train	60	0.069	90	35	0.9	0.93954
13	Train	60	0.078	90	35	2.86	2.24048
14	Train	60	0.089	90	35	5.284	6.16538
15	Train	70	0.038	90	35	0.32	0.28775
16	Train	70	0.047	90	35	0.43	0.35400
17	Test	70	0.058	90	35	0.56	0.63309
18	Validation	70	0.068	90	35	1.6	1.92338
19	Train	70	0.079	90	35	8.112	7.91750
20	Train	70	0.088	90	35	12.89	12.81275
21	Train	60	0.088	69.89	35	5.3	4.61353
22	Train	60	0.088	81	35	5.45	5.23502
23	Train	60	0.088	90.5	35	5.68	5.71054
24	Train	60	0.088	102	35	6.01	6.19181
25	Train	60	0.088	111	35	6.63	6.48973
26	Test	70	0.088	70	35	12.4	12.20766
27	Train	70	0.088	79.7	35	12.57	12.53870
28	Train	70	0.088	89.7	35	12.89	12.80585
29	Validation	70	0.088	101	35	13.5	13.02473
30	Train	70	0.088	110	35	14.6	13.14463
31	Train	60	0.088	90	30	5.95	6.20436
32	Train	60	0.088	90	35	5.69	5.68715
33	Validation	60	0.088	90	40	5.52	5.18159
34	Test	60	0.088	90	45	5.38	4.69325
35	Train	70	0.088	90	30	12.91	13.11987
36	Train	70	0.088	90	35	12.31	12.81275
37	Train	70	0.088	90	40	12.02	12.44150
38	Train	70	0.088	90	45	11.88	11.99746

(The VMD experiment was carried out in Jimei University [24].)

References

[1] Shirin Gh. Lovineh, Morteza Asghari, Bita Rajaei, Numerical simulation and theoretical study on simultaneous effects of operating parameters in vacuum membrane distillation, Desalination 314 (2013) 59–66.

[2] FeifeiShao, Changqing Hao, Lei Ni, Yufeng Zhang, Runhong Du, Jianqiang Meng, Zhen Liu, Changfa Xiao, Experimental and theoretical research on N-methyl-2-pyrrolidone concentration by vacuum membrane distillation using polypropylene hollow fiber membrane, Journal of Membrane Science 452 (2014) 157–164.

[3] Hong wei Fan, Yuelian Peng, Application of PVDF membranes in desalination and comparison of the VMD and DCMD processes, Chemical Engineering Science 79 (2012) 94–102.

[4] Jason Woods, John Pellegrino, Jay Burch, Generalized guidance for considering pore-size distribution in membrane distillation, Journal of Membrane Science 368 (2011) 124–133.

[5] S. Soukane, S. Chelouche, M.W. Naceur, A ballistic transport model for vacuum membrane distillation, Journal of Membrane Science 450 (2014) 397–406.

[6] A.O. Imdakm, M. Khayet, T. Matsuura, A Monte Carlo simulation model for vacuum membrane distillation process, Journal of Membrane Science 306 (2007) 341–348.

[7] Guy Ramon, Yehuda Agnon, Carlos Dosoretz, Heat transfer in vacuum membrane distillation: Effect of velocity slip, Journal of Membrane Science 331 (2009) 117–125.

[8] Jung-Gil Lee, Woo-Seung Kim, Numerical modeling of the vacuum membrane distillation process, Desalination 331 (2013) 46–55.

[9] S.M. Shim, J.G. Lee, W.S. Kim, Performance simulation of a multi-VMD desalination process including the recycle flow, Desalination 338 (2014) 39–48.

[10] Guangzhi Zuo, Guoqiang Guan, Rong Wang, Numerical modeling and optimization of vacuum membrane distillation module for low-cost water production, Desalination 339 (2014) 1–9.

[11] Chel-Ken Chiam, Rosalam Sarbatly, Vacuum membrane distillation processes for aqueous solution treatment—A review, Chemical Engineering and Processing 74 (2013) 27– 54.

[12] M. Khayet, C. Cojocaru, Artificial neural network modeling and optimization of desalination by air gap membrane distillation, Separation and Purification Technology 86 (2012) 171–182.

[13] M. A. Greaves, I. M. Mujtaba, M. Barolo, A. Trotta and M. A. Hussain, Neural network approach to dynamic optimisation of batch distillation – Application to a middle-vessel column, Transaction of IChemE 81 (2003) Part A 393–401.

[14] I. M. Mujtaba and M. A. Hussain, eds., Application of Neural Network and Other Learning Technologies in Process Engineering, Imperial College Press, London (2001) pp424.

[15] M. Barello, D. Manca, R. Patel and I.M. Mujtaba, Neural network based correlation for estimating water permeability constant in RO desalination process under fouling, Desalination 345 (2014) 101–111.

[16] B. Sarkar, A. Sengupta, S. De, S. DasGupta, Prediction of permeate flux during electric field enhanced cross-flow ultrafiltration - A neural network approach, Sep. Purif. Technol. 65 (3) (2009) 260–268.

[17] M.T. Hagan, H.B. Demuth, M. Beale, Neural Network Design, PWS Publishing Co., Boston, 1996.

[18] STATISTICA Electronic Manual.

[19] Yongqing Wang, Zhilong Xu, Noam Lior, Hui Zeng, Experimental investigation of a solar thermal-driven vacuum membrane distillation desalination system, Proceedings of ECOS 2013.

[20] M. Tavakolmoghadama, Mohammadali Safavi, An optimized neural network model of desalination by vacuum membrane distillation using genetic algorithm, Procedia Engineering 42 (2012) 106–112.

[21] STATISTICA software: http://www.statsoft.com/.

[22] Q. Kuang, L. Li, L. Min, Y. Ding, Desalination of Luobupo bitter and salty water by vacuum membrane distillation, Membrane Science and Technology 27 (4) (2007) 46–49 (In Chinese).

[23] M. Barello, D. Manca, R. Patel, I. M. Mujtaba, Operation and Modeling of RO Desalination Process in Batch Mode, In Computer Aided Chemical Engineering- 33, Klemes et al. (eds.), 451–456, 2014.

[24] Wang, Yongqing, Zhilong Xu, Noam Lior, Hui Zeng, An experimental study of solar thermal vacuum membrane distillation desalination, Desalination and Water Treatment 2014.